Estimating transport in Makassar Strait

Roxana C. Wajsowicz[a],[*],[1], Arnold L. Gordon[b,c], Amy Ffield[b], R. Dwi Susanto[b]

[a] *Department of Meteorology, University of Maryland, 3433 Computer and Space Science Building, College Park, MD 20742, USA*
[b] *Lamont-Doherty Earth Observatory of Columbia University, P.O. Box 1000, Rt. 9W, Palisades, NY 10964, USA*
[c] *Department of Earth and Environmental Science, Columbia University, Palisades, NY 10964, USA*

Abstract

Monthly averaged current meter data from two moorings in Labani Channel are examined, and a method, based on fitting normal modes, is developed to estimate the transport through Makassar Strait. The data span a depth range from about 210 to 1500 m and a time period from November 1996 to July 1998. They show monthly averaged southward currents in excess of 50 cm s^{-1} at 250 m, and episodes ranging from 1–6 months of 5–10 cm s^{-1} northward flow below 600 m. Estimates of the along-channel flow above and below the data record are made by fitting normal vertical modes, derived from climatological buoyancy frequency profiles, to the data. Tests of the fitting method show that the depth-averaged value is recovered well for profiles truncated between 200 and 250 m, but that the baroclinic structure cannot be recovered if more than the upper ~ 50 m of data are missing. However, for some almost full-depth acoustic Doppler profiles taken in Makassar Strait, the reconstructed flow averaged over the upper 250 m is typically found to lie within the bounds provided by the method. The estimated mean depth-integrated transport for 1997 is 6.4 Sv southwards with upper and lower bounds of 16.0 and 4.7 Sv respectively. Over the upper 250 m, the estimated mean transport for 1997 is 2.0 Sv southwards with upper and lower bounds of 9.7 and 0.8 Sv, respectively. The upper (lower) bounds are given by a normal mode reconstruction in which the first (third) baroclinic mode dominates the profile for much of the year; for the best estimate, the second baroclinic mode dominates the profiles through most of the year. The estimated mean net transport range for 1997 encompasses the earlier range published by Gordon et al. (Geophys. Res. Lett. 26 (1999) 3325), where empirical formulae were used to extrapolate the current profiles to the sea surface. The normal-mode reconstruction of the flow, temperature data from T-pods on the western Labani Channel mooring, and temperature and zonal wind data from the TAO moorings in the equatorial Pacific Ocean, provide a consistent description of cool, upwelling (warm, downwelling) baroclinic Rossby waves being scattered into the Indonesian archipelago as the equatorial zonal winds collapse (intensify) at the onset of El Niño (La Niña).

---

*Corresponding author. Tel.: +1-301-405-5396; fax: +1-301-314-9482.

E-mail address: roxana@atmos.umd.edu (R.C. Wajsowicz).

[1] Also affiliated with the Earth System Science Interdisciplinary Center, University of Maryland, College Park.

1. Introduction

Makassar Strait between Kalimantan and Sulawesi is thought to be the main pathway of a mean flow between the western equatorial Pacific Ocean and the eastern Indian Ocean, namely the Indonesian throughflow (e.g. Gordon and Fine, 1996; Wajsowicz, 1996). Current

meter moorings located at (2°52′S, 118°27′E) and (2°51′S, 118°38′E), henceforth referred to as MAK1 and MAK2, respectively, see Fig. 1, recorded currents in the Strait from the end of November 1996 until July 1998 and February 1998, respectively, as part of the Indonesia–US ARLINDO program. Very strong semi-diurnal and diurnal tides in the Strait presented numerous problems of which the most unfortunate was flooding of the upward-looking acoustic Doppler current profilers (ADCPs) attached to the moorings at 180 m (zero-wire angle), so that only a brief three-month record from the eastern mooring was recovered; further details of the moorings and recovered data are given in Gordon and Susanto (1999) (GS99 hereafter).

GS99 overcame the problem of data loss over the upper 250 m in their transport estimate by assuming three simple extrapolations for the upper layer along-channel current: (A) the mean thermocline shear is extrapolated to the sea surface, (B) the flow above the shallowest Aanderaa current meter equals the flow at that current meter, and (C) the along-channel speed decreases linearly from the shallowest Aanderaa current meter to zero at the surface. As no cross-sectional information was available on the flow, GS99 assumed that the velocity was horizontally uniform over the western half of the channel equaling the MAK1 velocity, and over the eastern half of the channel equaling the MAK2 velocity above 800 m (the deepest MAK2 meter was at 750 m). Below 800 m, the velocity was assumed horizontally uniform across the channel equaling the MAK1 velocity. The velocity was assumed to decrease linearly below the deepest current meter at 1500 m to zero at the bottom (2137 m). The estimated mean total transports through the Strait for 1997 were 11.3,
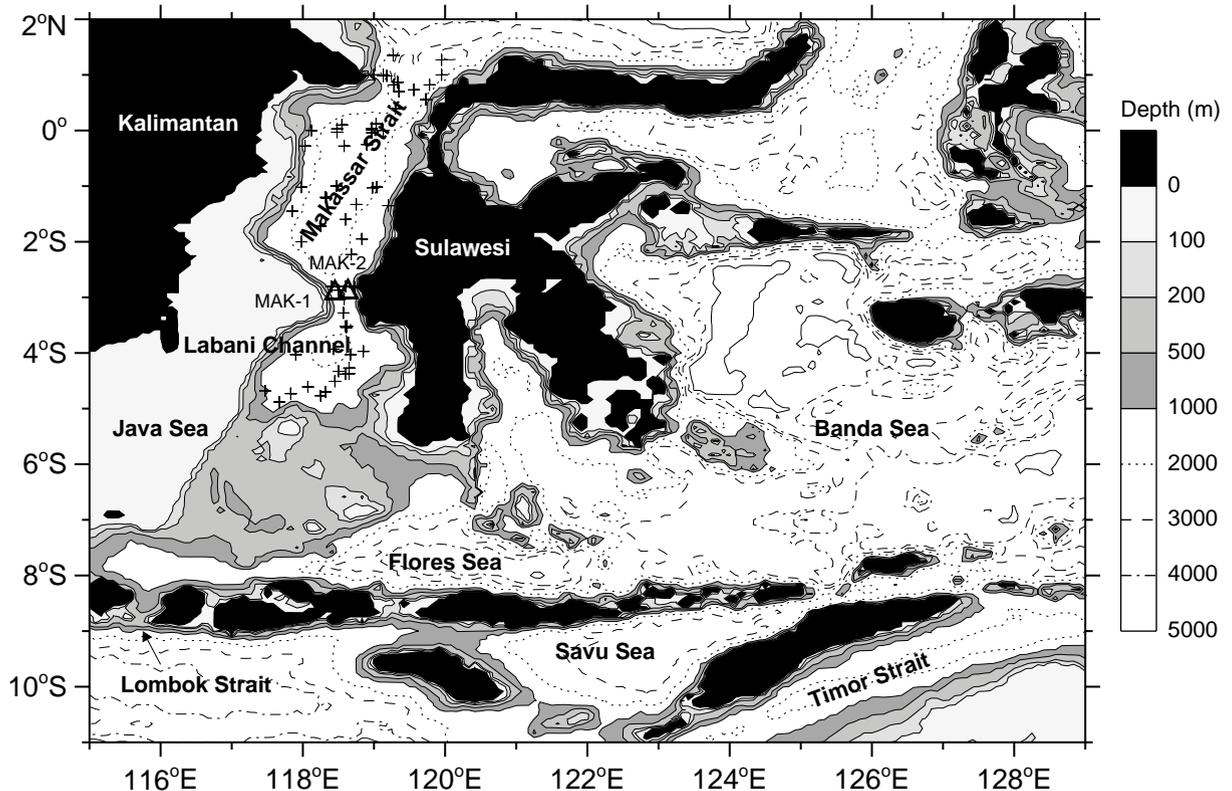
Fig. 1. Locations of the ARLINDO current meter moorings (triangles labeled MAK1 and MAK2) and of temperature and salinity stations from WODB98 (crosses), and bathymetry of Makassar Strait and surrounds.

9.3 and 6.6 Sv (1 Sv $\equiv 10^6$ m^3 s^{-1}), respectively, for profiles (A)–(C). Using a mixture of the profiles (Profile D: A in the boreal summer, C in winter, and B during the transition months), to represent seasonal variability, Gordon et al. (1999) derived a mean of 9.2 Sv.

Here, the mooring data are re-examined to see whether more information on the upper layer structure can be recovered by fitting normal vertical modes derived from the classical equation (Gill, 1982), using buoyancy frequencies for Makassar Strait. Knowledge of the upper layer structure is very important in determining the amount of heat transported by the throughflow into the Indian Ocean. It also affects how the throughflow interacts with the atmosphere over the Indian Ocean (Wajsowicz, 2002). The success with which severely truncated velocity profiles can be reconstructed using a normal mode fit has been examined using almost full-depth profiles obtained during an ARLINDO cruise in Makassar Strait, and a range of test profiles. New transports estimates with error estimates are made using the normal mode reconstructions of the velocity profiles. The transports do not differ substantially from those of Gordon et al. (1999), but the estimated error due to data loss over the upper 200 m is much greater; neither method provides absolute upper and lower bounds.

2. Reconstructing velocity profiles by fitting normal modes

If the functions $\{p_n(z)\}$ form a complete orthonormal set, then any piecewise continuous velocity profile $\mathbf{u}(z; x, y, t)$ is wholly described by them, i.e.

$$\mathbf{u}(z) = \sum_{n=0}^{\infty} \mathbf{u}_n p_n(z), \qquad (2.1a)$$

where

$$\mathbf{u}_n = \int_{-H}^{0} \mathbf{u} p_n \, \mathrm{d}z \bigg/ \int_{-H}^{0} (p_n)^2 \, \mathrm{d}z. \qquad (2.1b)$$

The task is to find a suitable set $\{p_n\}$. If the equations of motion are linear, and momentum dissipation expressible in the form

$A\nabla_h^2 \mathbf{u}$, $\partial_z[(\kappa/N^2)\partial_z \mathbf{u}]$, where N is the buoyancy frequency, then solutions can be found in separable form, i.e. $\mathbf{u}_n(x, y, t)p_n(z)$, where $\mathbf{u}$ satisfies the linear, shallow-water equations for wavespeed c_e and the vertical modes p_n satisfy

$$\frac{\mathrm{d}}{\mathrm{d}z}\left\{\frac{1}{N^2}\frac{\mathrm{d}p}{\mathrm{d}z}\right\} = -\frac{1}{c_e^2}p, \qquad (2.2a)$$

subject to

$$p_z = 0 \quad \text{at } z = -H, 0, \qquad (2.2b)$$

(e.g., McCreary, 1981; Wajsowicz and Gill, 1986; Gill, 1982, in which sections 6.11, 6.13 gives a description of normal modes in a continuously stratified fluid with examples of classic problems and their solutions).

Makassar Strait is about 2000 m deep along its length and about 200 km wide except in Labani Channel, where it reduces to about 50 km, see Fig. 1. The reduction in width is not particularly abrupt, and so the horizontal scale of the motion is expected to be much larger than the vertical scale for low-frequency ($\omega \ll f$) motions. This is borne out by the similarity in vertical and in temporal structures of the data from the moorings discussed in the next section, which are about 15 km apart. Therefore, a possible choice for the $\{p_n\}$ are the classical normal modes for some N^2 representative of Makassar Strait. It is important to note that in choosing these p_n, it is not supposed that the coefficients in (2.1a) are functions of x, y, t satisfying the shallow-water equations.

2.1. Normal modes in Makassar Strait

Buoyancy frequency profiles for Makassar Strait are calculated from concurrent temperature and salinity data in the National Oceanographic Data Center's (NODC) World Ocean Data Base 1998 (WODB98 hereafter) (Boyer et al., 1998a, b, c). Only stable profiles ($N > 0$ for all z), and those extending to depths greater than 1000 m, see Fig. 2a are used. High-resolution buoyancy frequency profiles from data collected during the ARLINDO cruises in Makassar Strait confirm the spread of these historical profiles (Fig. 2b). The profiles were averaged to produce a mean profile (Fig. 2c). Sensitivity of the normal mode structure to the
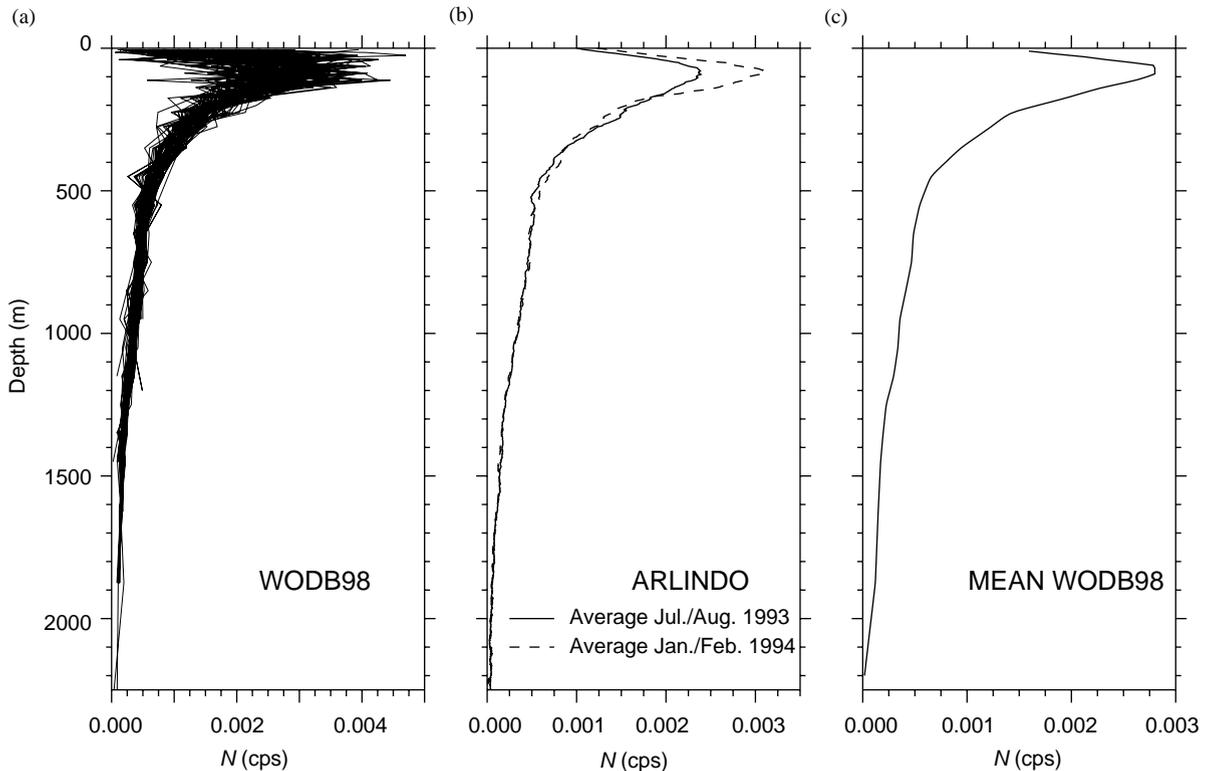
Fig. 2. Buoyancy frequency profiles for Makassar Strait using temperature and salinity profiles from: (a) NODC's WODB98 (minus 1993/1994 ARLINDO data), (b) ARLINDO cruises, and (c) mean of (a) and (b). Only stable profiles which extend over a depth of greater than 1000 m are plotted.

buoyancy frequency profile was explored, and Fig. 3 illustrates the spread that is obtained for the structure of the first three baroclinic modes; they have been normalized so that $\int_{-H}^{0}(p_n)^2 \, dz = 1$. The success with which the full-depth velocity profiles can be recovered depends on how much of the structure of the modes, i.e. their zero-crossings and extrema, lie within the data range, and the extent to which the data range captures the important features of the flow. The modes from the ARLINDO July/August N^2 appear to have most structure within the data range. The modes from the mean WODB98 appear to have the least, but this could well reflect the true situation. In the following, reconstructions are derived based on these two sets.

The structure of the normal p_n modes and baroclinic wavespeeds for the MAK2 mooring are indistinguishable from those calculated for the MAK1 site over the relevant depth; the same buoyancy frequency profile is used, but the lower boundary condition is applied at 1611 m depth rather than 2137 m depth in Eq. (2.2).

2.2. Fitting method

As current profiles were not obtained for the entire water column, the data cannot be projected uniquely, according to (2.1), onto the normal p_n-modes. Also, as the modes are not necessarily linearly independent over the range of the data, a multi-variate, least-squares fit is not appropriate; the fit matrix may be almost singular, and so result in large errors on inversion. Hence, a simple, sequential fitting scheme is adopted. First, the best fit is found for the
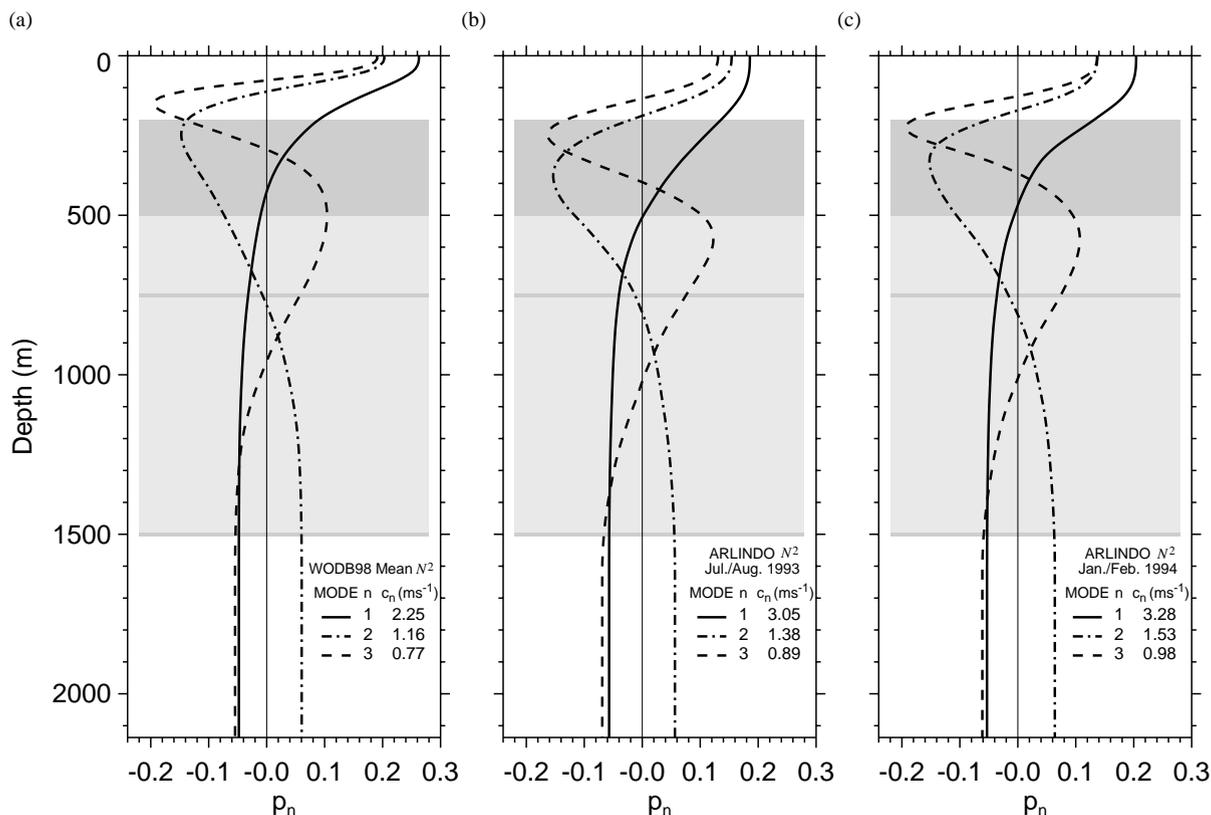
Fig. 3. Normalized p_n-eigenvectors for buoyancy frequency profiles (a) mean WODB98 in Fig. 2c, (b) ARLINDO July/ August 1993 in Fig. 2b, and (c) ARLINDO January/February 1994 in Fig. 2b. Wavespeeds for first three baroclinic modes are given on the plots. At MAK1 (MAK2), $H = -2137$ m (-1661 m), so barotropic mode wavespeed is 145 m s^{-1} (126 m s^{-1}). Depths spanned by MAK1 current meters are shaded dark gray; light gray denotes regions where the data are interpolated for the normal mode fitting. There was no current meter at 1500 m on MAK2.

first baroclinic mode using a least-squares criterion, then the best fit to the residual is found for the second baroclinic mode, and so on for the third, etc. Assuming the $n = 0$ mode is uniform with depth, i.e. barotropic, its coefficient is just the residual constant from the least-squares fit. The coefficients obtained are sensitive to the order in which the modes are fitted, and as expected for low-frequency ($\omega \ll f$) motions, most of the energy is contained in the first three baroclinic modes and the barotropic mode. Hence, these latter modes are the focus of the following analysis, and all six permutations of fitting order, i.e. $n = 1, 2, 3$, $n = 2, 3, 1$, etc., are considered.

2.3. Test profiles

Tests were made with thousands of profiles, generated by assigning coefficients randomly to each mode, adding up the components, and then removing the top portion of the profile down to observed depths. If a single baroclinic mode clearly dominates, then the recovery is good, even if as much as the upper 300 m of the profile are missing. However, if the profile is made up of baroclinic modes of similar magnitude, then the recovery can be poor, though the barotropic velocity is typically well recovered. A demonstration of the method's ability to recover the components is given in Fig. 4. The velocity profile (Fig. 4a) is the average of three
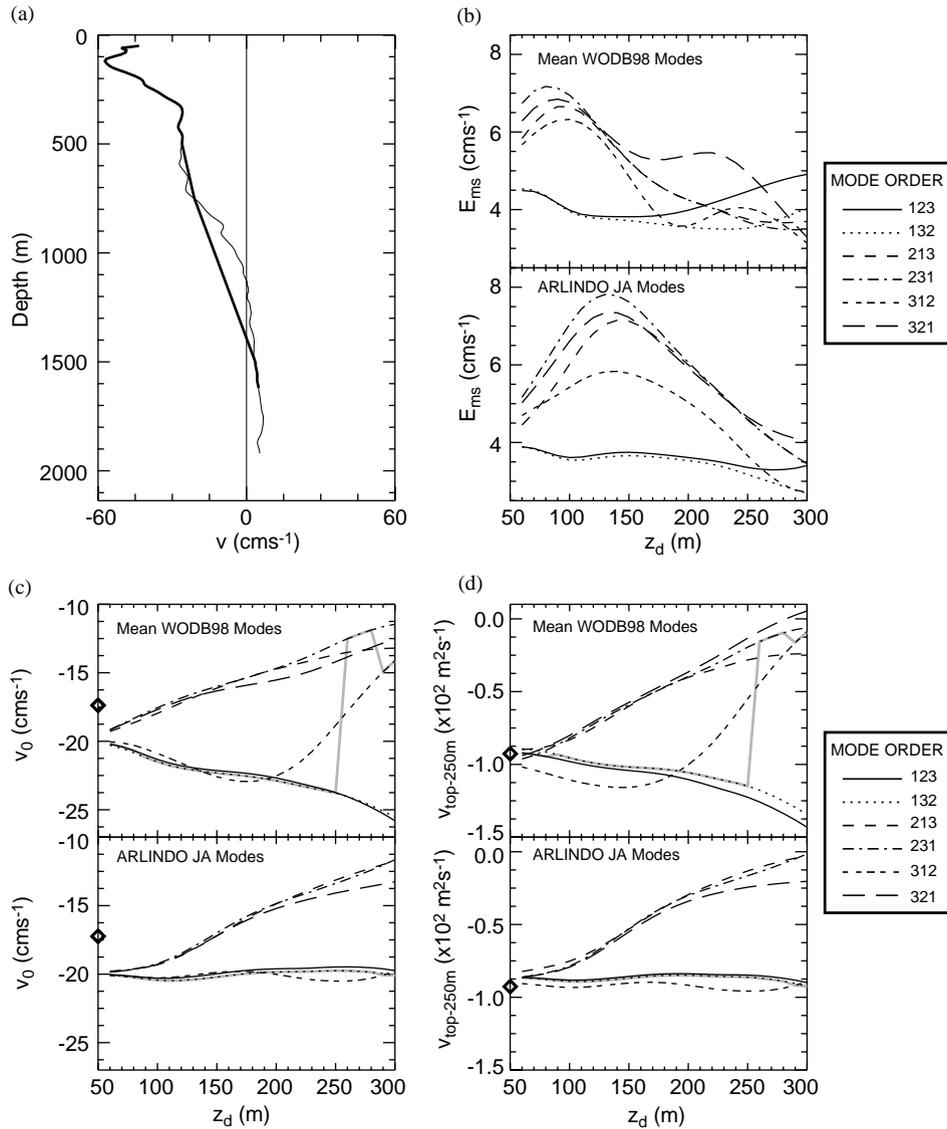
Fig. 4. (a) An almost full-depth current profile (thin line) obtained from averaging LADCP measurements at three sites at southern end of Makassar Strait; (solid line) profile obtained from interpolating between 500, 750 and 1500 m, mimicking interpolation MAK1/MAK2 current meter data later. Applying fitting method described in Section 2.2 to interpolated current profile between z_d and 1500 m yielded for each fitting permutation (b) r.m.s. errors, (c) reconstructed barotropic velocity, (d) reconstructed velocity integrated over upper 250 m, as a function of z_d. Results are for fitting mean WODB98 modes (upper panel) and ARLINDO July/August 1993 modes (lower panel). Light gray line denotes best fit, i.e. minimum r.m.s. error, for a given z_d in (b) and (c), and diamond on ordinate axis is result from fitting full profile (thin line in a).

almost-full-depth profiles from Makassar Strait taken using a Lowered Acoustic Doppler Current Profiler (LADCP) during the 1998 ARLINDO cruises. The data are available from about 50 to

2000 m. To mimic the ARLINDO current meter data, the profiles are linearized between 500 and 750 m, and 750 and 1500 m, and fitted between z_d and 1500 m. For the ARLINDO July/August 1993

modes of Fig. 3b, the best fit (minimum r.m.s error, Fig. 4b) is given by fitting the first baroclinic mode first for the range of z_d considered. Also the best-fit recovered barotropic speed (Fig. 4c), and speed integrated over the upper 250 m are approximately independent of z_d for this range. For the mean WODB98 modes, the best-fit is given by fitting the first baroclinic mode first for $z_d < 250$ m. For $z_d > 250$ m, the best-fit is given by other permutations, which have much reduced barotropic velocity and upper layer transport. For the MAK1/2 current meter data, described in the next section, $210\ \text{m} \leqslant z_d \leqslant 260$ m. These results suggest that in estimating the net transport and transport over the upper thermocline, upper and lower bounds are provided by the range spanned by the permutations.

3. Currents in Labani Channel, Makassar Strait

3.1. Direct current measurements from the ARLINDO program

The data from the current meters on the MAK1 and MAK2 moorings were projected onto the along-channel direction and filtered to remove the diurnal and semi-diurnal tides. The mooring blowover due to the semi-diurnal tide was sufficient that the upper three current meters spanned depths between about 250 and 500 m four times a day. The resulting data on a 10-m grid were described by Gordon et al. (1999). These data along with those from the meters at 750 and 1500 m (MAK1 only) were binned monthly (Figs. 5 and 6); linear interpolation has been used between 500 and 750 m, and 750 and 1500 m. There was some sway in the moorings due to lower frequency motions. For example, in July/August 1997, there was only good coverage up to 260 m from the MAK1 mooring, whereas in May/June 1997 and January 1998, good coverage was obtained up to 210 m. The MAK2 mooring gave good coverage up to 210–230 m.

Features of note in the monthly averaged data are

(i) Northward flow at depth in May 1997, from August 1997 to December 1997, and from June 1998 until the end of the data set in early July 1998. It lies below 600 m typically, but reaches above 400 m in October 1997 (Fig. 5a).

(ii) These occasions of pronounced reversed flow at depth are associated with strong vertical shear in the along-channel current anomalies (Fig. 5b).

(iii) The signal from MAK2 is similar to MAK1, but the currents are weaker typically.

(iv) Three months of data from the upward-looking ADCP on the MAK2 mooring (Fig. 6a) give northward flow near the surface from December 1996 to February 1997 inclusive, and a southward maximum of 55–70 cm s^{-1} at 190 m.

(v) The spread of over 10 cm s^{-1} found between the six 12-month-averaged profiles in Figs. 5b and 6b.

(vi) Three-monthly peak-to-peak variations in excess of 55 cm s^{-1} at around 400 m (Fig. 5b).

Feature (i) is quite surprising, and GS99 suggested it may be due to the influence of the 600 m sill at the southern end of Makassar Strait. There have been other reports of northward flow in Makassar Strait, and flow at depth. From the ASEAN current meter data collected from mid-June 1993 for a year, Aung (1995) reported a mean northward flow over the 12 months of 2–4 cm s^{-1} between about 700 and 1300 m on the northeastern side of Makassar Strait. He also found northward flow in the first half of the year of 12 cm s^{-1} at 400 m on the northeastern side and 2 cm s^{-1} at 1200 m on the northwestern side. However, below 1300 m, Aung (1995) found mean southward flow of 3.0–3.9 cm s^{-1} in the northern central section of the Strait. Wyrtki's (1961) investigation of the seasonal cycle documents a reversal of surface flow in the southern half of the Strait in October, but this more relates to feature (iv).

Feature (ii) is expected to show up as a significant change in relative amplitudes of the normal modes in the following, as it represents a quite dramatic change in vertical structure of the current. The flow through Makassar Strait is essentially that of the western boundary current of the Indo–Pacific basin, and therefore western

(a)
MAK1: Along-Channel Current

(b)
MAK1: Along-Channel Current Anomaly
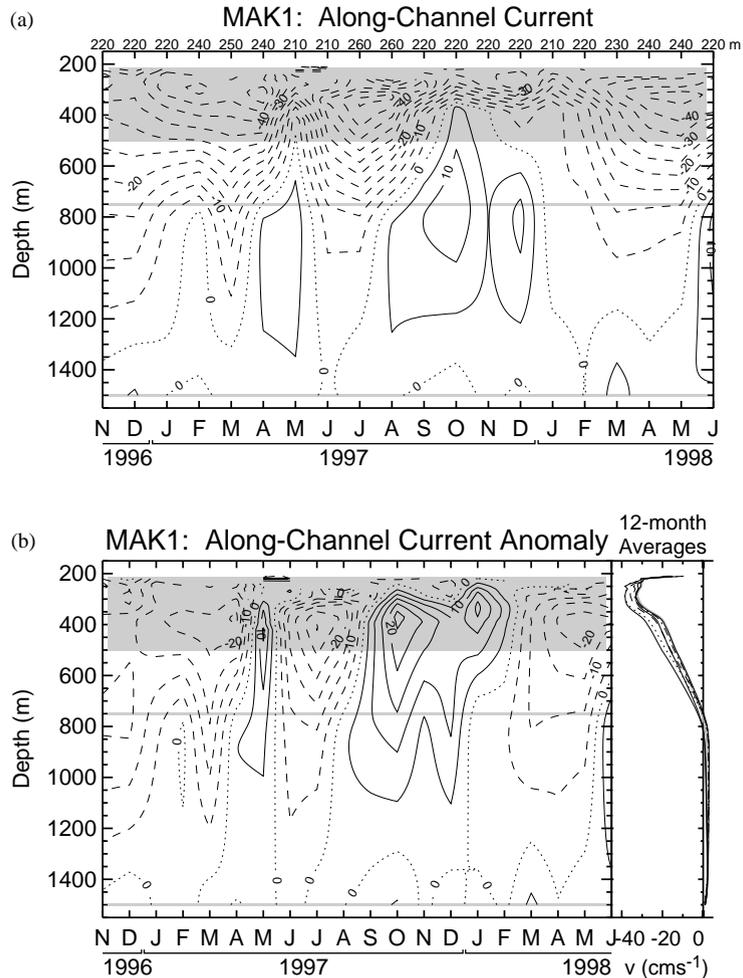
Fig. 5. (a) Monthly averages of along-channel current from MAK1 current meter data as a function of time (November 1996 to June 1998 inclusive) and depth; data are linearly interpolated between 500, 750 and 1500 m with dark gray shading denoting actual measurements. Uppermost depth of each monthly profile is given above upper abscissa. (b) Along-channel current anomalies relative to 12-month May 1997 to April 1998 mean; dark gray shading as in (a). Profiles for consecutive 12-month averages are plotted on the r.h.s.; solid gray line denotes May 1997 to April 1998 average. (Note, above 260 m, mean is not for whole 12 months.) Contour interval is 5 cm s^{-1}; positive values are denoted by solid lines, negative by dashed, and zero contour by a dotted line.

intensification of the current is to be expected as noted in (iii). It is likely that the intensification is enhanced as the western flank of the current accelerates around the bend in the Kalimantan coastline (see Chow, 1959). From Fig. 1, the eastern boundary of the channel is quite straight, but in the west, the channel is at the apex of a significant convex curve in the boundary defined by isobaths greater than 100 m. Regarding feature (iv), the distinct maxima and minima between 250

and 300 m seen in Figs. 5 and 6 might be assumed to represent the current core. It roughly corresponds to the depth of an extremum of the second or third baroclinic mode in Fig. 3. However, the first baroclinic mode has its extremum at the surface, and so, at times when it dominates, the main current core is expected to lie near the surface.

Feature (v) is a measure of a large interannual, or longer timescale, variability in the current,
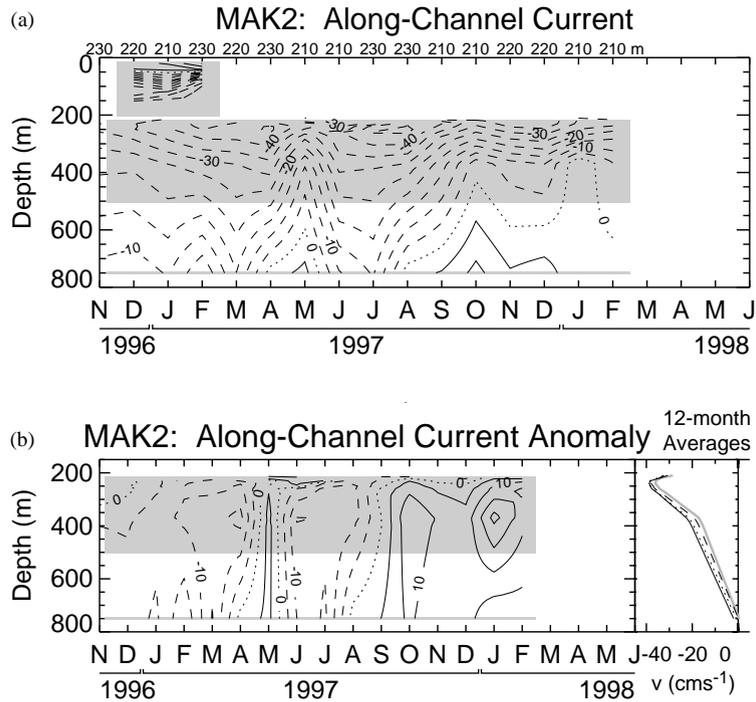
Fig. 6. As in Fig. 5, but for MAK2 current meter data. Also contoured in (a) is three months of ADCP data; instrument at 180 m (zero wire-angle). Anomalies in (b) are relative to March 1997–February 1998 mean.

which translates into significant net transport variations described in the next subsection. This large variability is matched by a very large approximately semi-annual variability of ± 25 cm s^{-1} on a mean current of 35 cm s^{-1}, feature (vi). There is little indication of annual period variability, which contrasts with Murray and Arief's (1988) findings in Lombok Strait to the south; estimates of transport through Lombok Strait from direct current measurements showed a dominant annual period.

Twelve-month averages indicate that the mean currents between ~ 330 and 750 m are about three-quarters of the strength at MAK2 compared with MAK1, (Fig. 7a). This is consistent with a western boundary layer width of about 70 km (suppose $u_1 = u_0 e^{-ax_1}$ and $u_2 = u_0 e^{-ax_2}$, then $a = \ln(u_1/u_2)/(x_2 - x_2)$, $x_2 - x_1 = 15$ km). Above ~ 330 m, the MAK2 along-channel speed increases relative to that at the MAK1 site, and is larger above about 260 m to the top of the record at 210 m. However, the data record is incomplete

above 260 m, and so the change in relative strength should be viewed with some caution.

The mean and linear trends in the time series are similar between the sites (Fig. 7b). However, the vertical structure of the linear trend is notably different from that of the mean. The relative monthly anomalies (Fig. 7c) are generally such that the along-channel speed at the MAK1 mooring is greater than at the MAK2 mooring, and such that the ratio of speeds is almost constant with depth below about 330 m. For most months, the ratio is around 0.7, as for the 12-month means; but for a few of the months, notably the monsoon transition months May 97, October 97, November 97, the ratio is around 0.2, consistent with an exponential boundary layer width of only 10 km. Above 330 m, the relationship shows a variety of different behaviors. The much narrower boundary layer scale for the monthly anomalies suggests a summation of signals propagating in opposite directions through the Channel trapped against opposite walls.
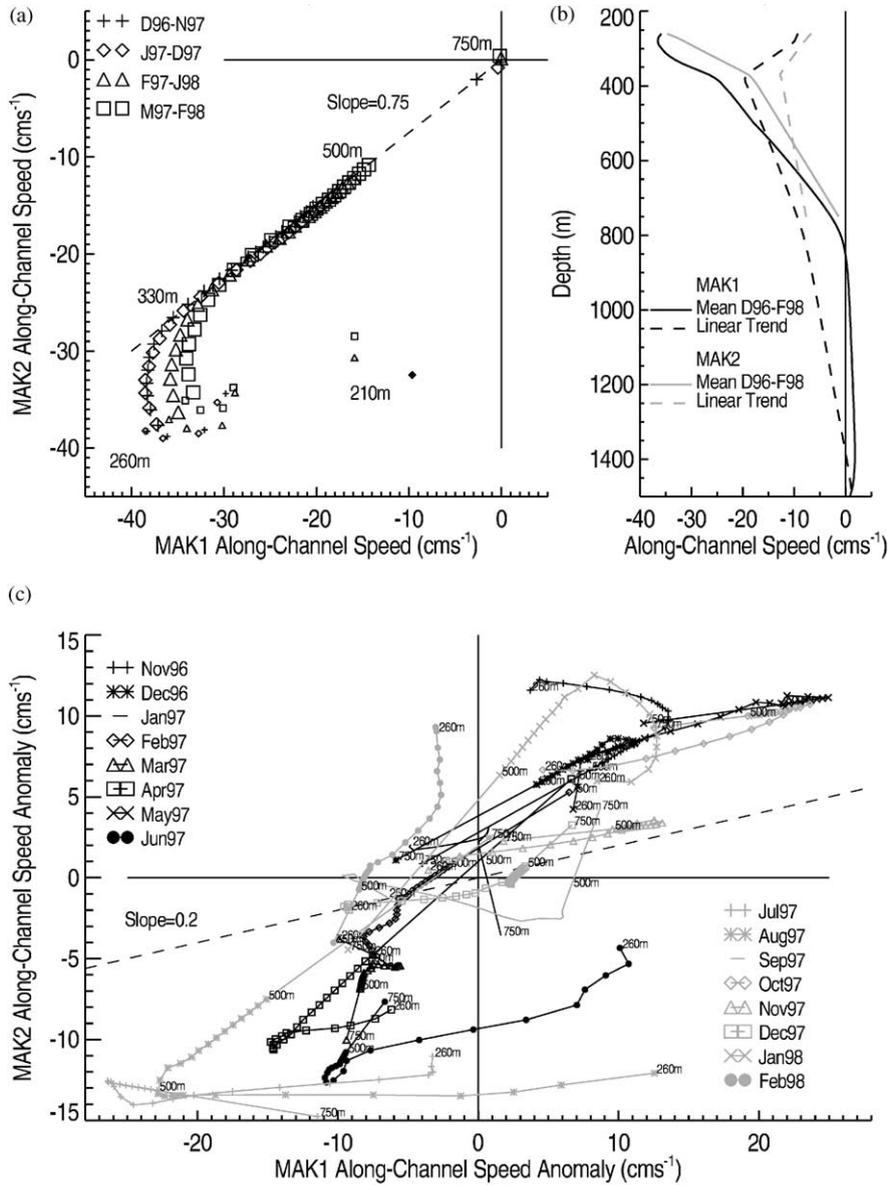
Fig. 7. (a) Relationship between annual mean along-channel speed at MAK1 vs. MAK2; line-style key for each 12-month average is given in top left-hand corner, (b) Mean of (solid) and linearly increasing trend (dashed) in MAK1 (black) and MAK2 (gray) data from December 1996 to February 1998. (c) Relationship between MAK1 and MAK2 along-channel current anomalies, obtained by subtracting the mean and linear trend plotted in (b); linestyles keys for each month are given in the top left and bottom right corners.

Fig. 7 confirms that although the bottom topography in the archipelago is complex, the horizontal scale of the monthly-averaged currents in Makassar Strait is large compared with the vertical scale, and so the normal mode sets derived in Section 2 are a reasonable choice of basis functions for fitting the data. In order to obtain a transport estimate from the mooring data, an assumption needs to be made about the cross-channel structure of the flow. From Fig. 7a, for

calculating the annual mean, an exponential variation with a decay scale of 70 km could be used for each depth, though the relationship may be different over the upper thermocline. For calculating seasonal and shorter timescale transport variability, Fig. 7b shows that this simple algorithm is likely to be even more approximate.

Taking into account all of these facts, in the following, a simple transport estimate is made based on the assumption that the along-channel velocity is horizontally uniform over a rectangular channel of equivalent cross-section; most of the estimates use the MAK1 along-channel speed only. Finally, Fig. 7b indicates that it would be better to recover the mean and monthly anomalies separately; the mean is a complex combination of modes, but the low-frequency ($\omega \ll f$) variability is more likely to be dominated by the first or second baroclinic modes. However, the tests described in Section 2 emphasize that a cut-off of ~ 220 m versus 260 m could be crucial in the success of the fitting. Some trials were made of the two schemes, and it was decided to reconstruct the along-channel velocity at each mooring for each individual month.

3.2. Projection onto normal vertical modes

The results from applying the fitting scheme described in Section 2.2 to the individual monthly averaged profiles from the MAK1 current meter are similar for both sets of normal modes shown in Fig. 3a and b. However, the mean and amplitude of the monthly variability are up to 50% larger for the permutations in which the first baroclinic mode is fitted first for the mean WODB98 modes. For these latter modes, fitting the second baroclinic mode first gives the best fit in most months (Fig. 8a) whereas for the ARLINDO July/August modes, fitting the first baroclinic mode first gives the best fit for just over half of the twenty months (Fig. 8b). As suggested earlier, the occasions on which there is a significant reversal in flow at depth correspond to the collapse in magnitude of the second baroclinic mode coefficient, and an increase in the magnitude of the first baroclinic mode coefficient (not shown), or roughly, a switch

to the best-fit being given by fitting the first baroclinic mode first rather than the second.

To convert the recovered along-channel velocity into transport estimates, several estimates of the geometry of the cross-section were considered (Fig. 9). GS99 and Gordon et al. (1999) used the Smith and Sandwell (1997) profile in the formula $0.5 \sum_{k=1} [v_1(k) + v_2(k)] W(k) d$, where $W(k)$ is the width of the channel at depth k, $d = 10$ m, and v_1, v_2 are the respective velocities at the MAK1 and MAK2 moorings assuming empirical profiles above and below the highest and lowest current meter, as described in Section 1. The cross-section from the ship's echosounder is used in the calculations presented here. The net transport is calculated as $\bar{V}A$, where A is the cross-sectional area, and $\bar{V}$ is the recovered barotropic velocity. Layer transport is calculated according to the formula $[\sum_{k=k_1}^{k_2} V_1(k)] d W_{\text{eff}}$, where V_1 is the reconstructed velocity from the MAK1 data at intervals of $d = 10$ m, and W_{eff} is effective width of the channel assuming a rectangular cross-section, i.e. $W_{\text{eff}} = A/D$, where $D = 2137$ m, the channel depth at the MAK1 mooring.

Placing the months sequentially provides an approximate transport time series. The net transport time series is similar to that calculated by Gordon et al. (1999); transport is southwards and of O(10 Sv), larger during the first half of the record than the second half though strengthening again towards the end of the record, and reduced in May 1997. Both Fig. 8a and b suggest that a significant fraction of the transport occurs below 250 m. For comparison, and to provide encouragement that the transports recovered give a fair estimate, also plotted in Fig. 8 is the net and upper thermocline Indonesian throughflow from an almost-global ocean GCM hindcast performed by Rosati and Harrison at the NOAA/Geophysical Fluid Dynamics Laboratory, Princeton. The GCM was forced by realistic surface fluxes and assimilated all available temperature data between 500 m and the surface over the 20 years of the hindcast from the beginning of 1980 to the end of 1999; further details are given at http://nomads.gfdl.noaa.gov. The net transport time series from the GCM hindcast lies roughly within the bounds provided by the permutations for both
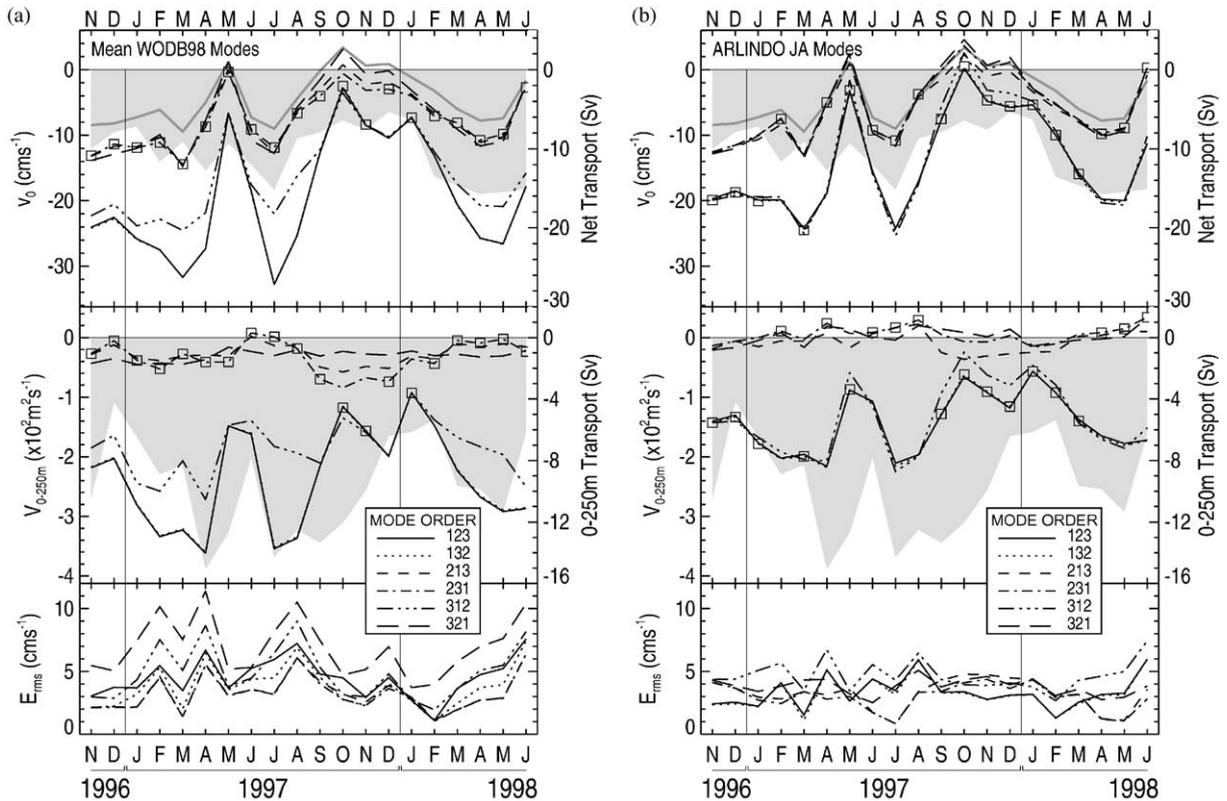
Fig. 8. (a) Fitting WODB98 normal modes to MAK1 along-channel current meter data gives reconstructed barotropic velocities (top panel), reconstructed velocities integrated over upper 250 m (middle panel), and r.m.s. errors (bottom panel) for each month and for each permutation; best-fit denoted by boxes. Transport axes are given on r.h.s. assuming an equivalent rectangular cross-section based on cross-channel depth measurements from a ship echosounder. Light gray histogram in top and middle panels denotes Indonesian throughflow transport time series from a GFDL ocean GCM hindcast with assimilation. Bold gray line in top panel is observed 260–1500 m layer transport. (b) Same as (a), but for fitting ARLINDO July/August 1993 modes to data.

sets of modes, and has the basic features noted above. However, in the GCM, most of the Indonesian throughflow is carried over the upper 250 m, and so the modeled transport over the upper 250 m lies on or above the upper bound of the reconstruction using the mean WODB98 modes, and well above that for the ARLINDO July/August 1994 modes. A possible explanation for this difference in vertical distribution of transport is the lack of shallow sills in the Indonesian throughflow region in the GCM, supporting GS99's suggested explanation for feature (i).

The reduction in throughflow transport during the 1997/1998 El Niño is expected from Clarke (1991), as a relaxation in zonal winds over the equatorial Pacific Ocean generates westward-propagating, cool, upwelling Rossby waves, which partially scatter through the archipelago. Interestingly, the time series of the normal mode coefficients (not shown) are consistent with this explanation, and Anderson and Gill's (1975) theory for the response due to a change in wind stress with a rapid barotropic response followed by a slower baroclinic response signed to cancel the barotropic velocity at depth.

The normal mode fitting method suggests that the estimated error in calculating the net transport from the limited observations is much larger than given by Gordon et al.'s (1999) A,B,C profile fit; it
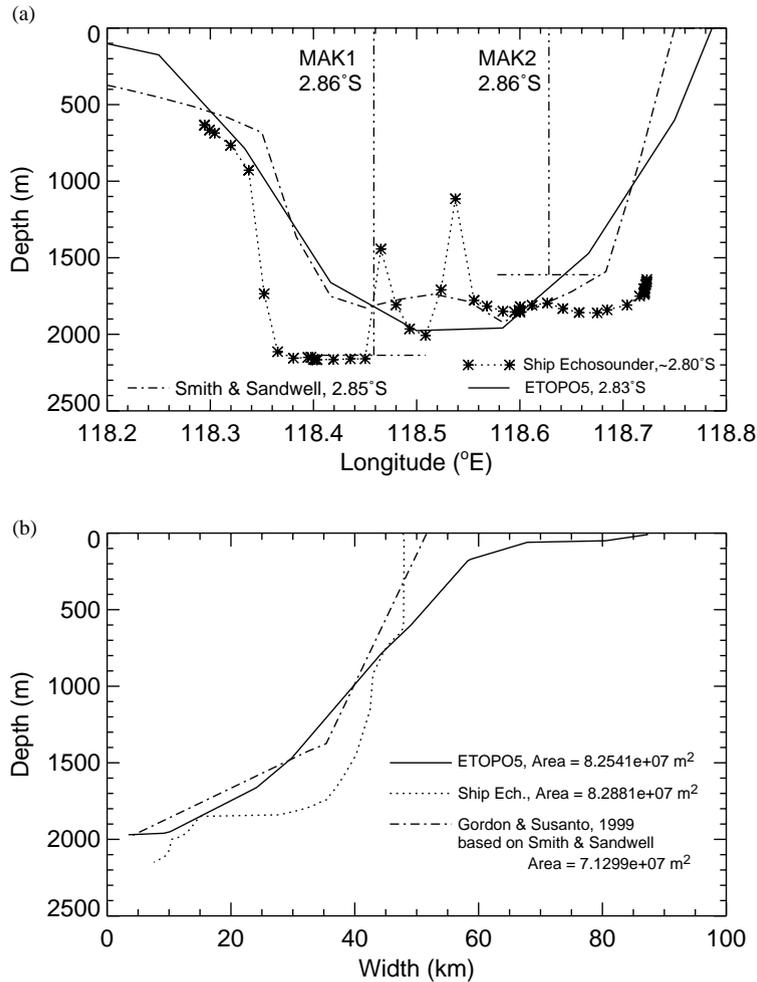
Fig. 9. (a) Cross-sectional geometry of Labani Channel from the Smith and Sandwell (1997) topographic data set, ETOPO5 (NOAA, 1988), and from a ship echosounder, at approximate latitude of MAK current meter moorings; positions of MAK1 and MAK2 moorings are overlain. (b) Width of channel as a function of depth for each data set.

is as large as 15 Sv for a couple of months. A series of 12-month means of the reconstructed net transport for the 20-month data record gives best-fit values lying between 5 and 7 Sv; see Fig. 10a, for both sets of modes. Minimum 12-month means from the normal mode reconstruction lie in the range 3–5 Sv (2–4 Sv), and maximum means from 13 to 17 Sv (9−12 Sv) for the mean WODB98 modes (ARLINDO modes); Vranes et al. (2002) found 12-months means ranging from 7.7 to 9.9 Sv for Profile D. Gordon et al. (1999) gave an estimate for net transport in

1997 of 9.3 ± 2.5 Sv; the upper and lower bounds are due to the uncertainty in the profile over the upper 250 m rather than instrument error or error due to lack of knowledge of the cross-sectional variation. From Fig. 10a, the normal-mode method gives an estimate of 6.4 Sv with upper and lower bounds of 16.0 and 4.7 Sv, respectively. For transport over the upper 250 m, the best-fit 12-month average is about 2 Sv with a minimum of 0.5 Sv (0.5 Sv northwards) and maximum in the range 9–11 Sv (5–6 Sv) for the mean WODB98 modes (ARLINDO modes).
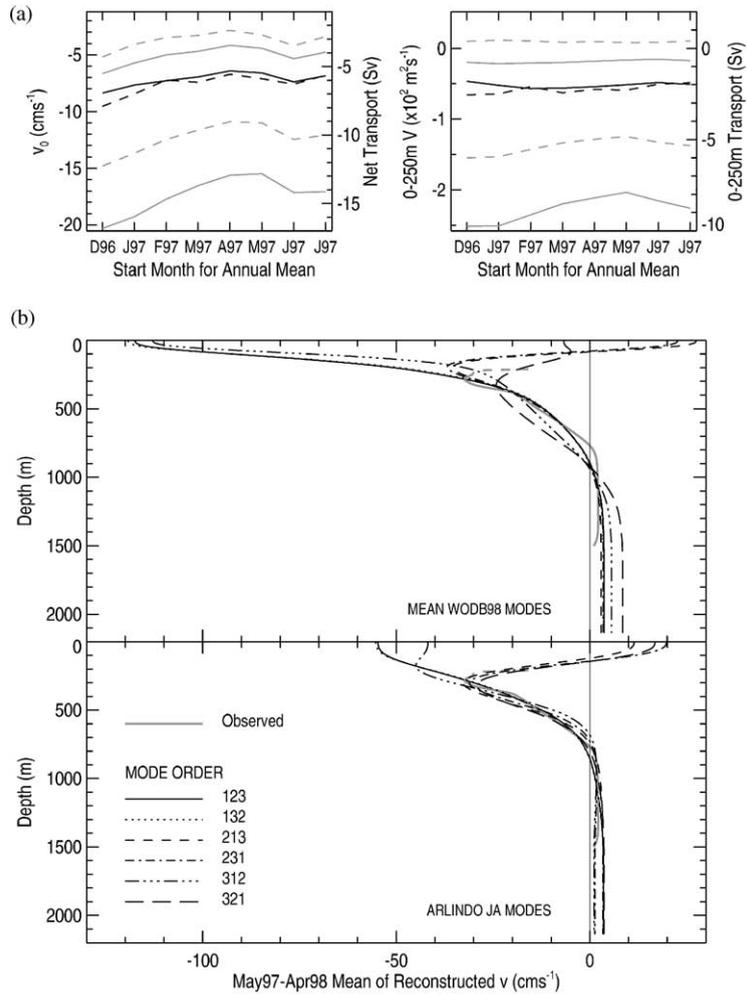
Fig. 10. (a) Annual means of net transport (l.h.s.) and transport over upper 250 m (r.h.s) obtained by averaging 'best-fits' to MAK1 profiles for 12 months with start dates from December 1996 to July 1997; solid (dashed) black line using mean WODB98 (ARLINDO July/August) modes. Light gray lines denote corresponding 12-month averages of minimum and maximum recovered values each month. (b) Example of vertical structure obtained by averaging velocity recovered for each permutation order from May 1997 to April 1998 is plotted; upper (lower) panel using mean WODB98 (ARLINDO July/ August) modes.

The vertical structure of 12-month means obtained from the reconstructed velocity profiles, (see Fig. 10b for example of May 1997 to April 1998) show that when the second baroclinic mode dominates the reconstructed profile, there is weak (20 cm s^{-1}) *northward* flow at the surface. Fitting the first baroclinic mode first yields profiles with a large (55–150 cm s^{-1}) *southward* surface flow. The profiles in Fig. 10b are obtained by averaging the recovered monthly profiles, and not by fitting

the profile obtained from averaging the observations shown in Fig. 5b. The ARLINDO July/ August modes appear to capture better the sharp reversal in the current gradient above 300 m, but this reversal needs to be treated with caution, as the data set is incomplete over these depths for the 12 months.

An equivalent analysis performed on the MAK2 current meter data yielded similar results to the MAK1 analysis (Fig. 11) even though a first
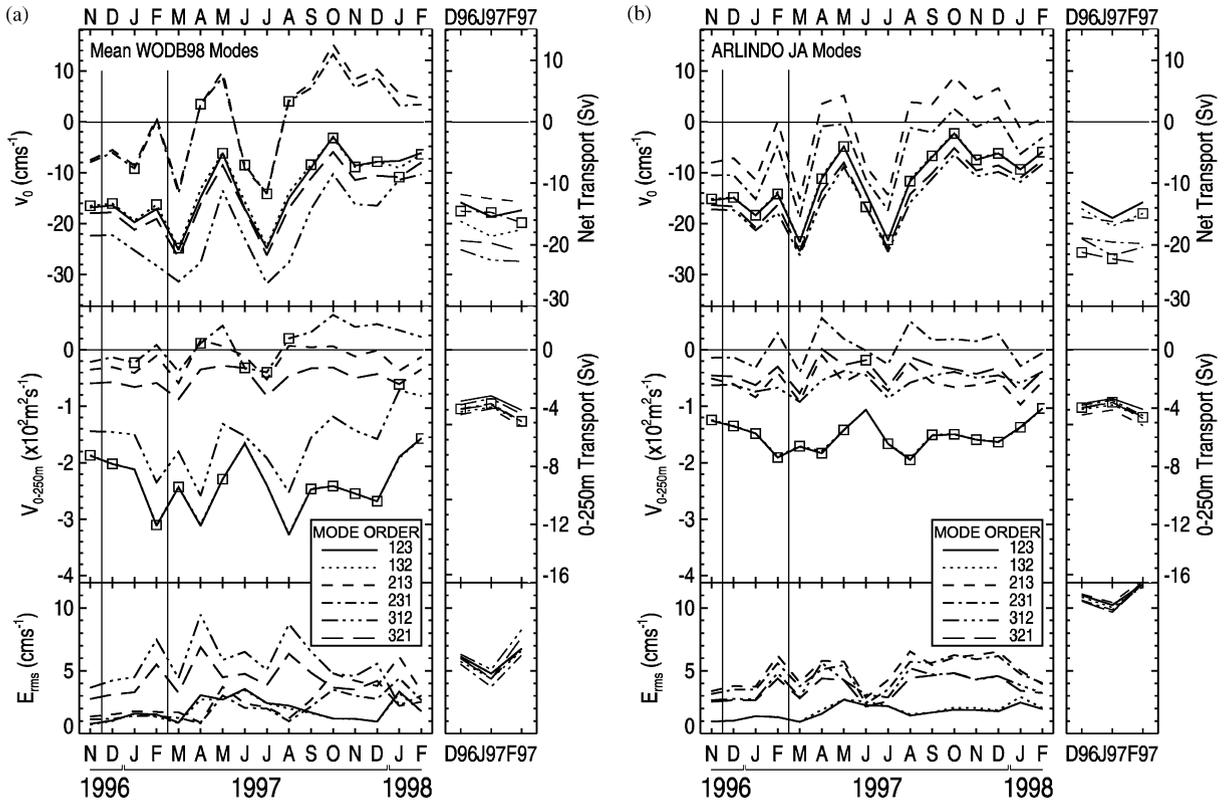
Fig. 11. As in Fig. 8, but from fitting MAK2 current meter data. Plots for three months on r.h.s. of (a) and (b) are from fitting available ADCP (20–200 m) as well as current meter data.

baroclinic mode dominated flow is favored. The additional constraint imposed by fitting three months of ADCP data as well is also shown in Fig. 11. As expected, the transport over the upper 250 m for both sets of modes is rigorously constrained to give ∼ 4 Sv. The net transports are also brought more into agreement with values lying between 12 and 24 Sv. For the normal modes derived from the mean WODB98 buoyancy frequency profiles, including the ADCP data between 20 and 200 m serves to constrain the fit better rather than give vastly different values. However, for the normal modes derived from the high-resolution CTD casts taken during the ARLINDO cruises, inclusion of the ADCP data, showed that these modes had possibly underestimated the net transport.

There is further observational evidence to support northward surface currents, suggested by

the prominence of the second baroclinic mode in the reconstruction, at least during part of the year. Murray and Arief (1988) reported current meter measurements from moorings in the vicinity of Lombok Strait to the south of Makassar Strait, see Fig. 1. Their time series for current meters at 35, 75, 300 and 800 m for January to May 1985 show similar features to the ARLINDO data. In February and March, there is northward flow of a few cm s^{-1} at 800 m with larger southward flow above at 300 m. The flow over the upper 100 m is mainly southwards, but there are 10–15 day episodes in February through April when large northward currents were recorded. Currents in the upper 100 m ranged from 50 to 100 cm s^{-1}, whereas at 300 m, they rarely exceeded 20 cm s^{-1}. Also consistent with the ARLINDO data was the observed collapse of the surface currents from October 1985 until the end of the
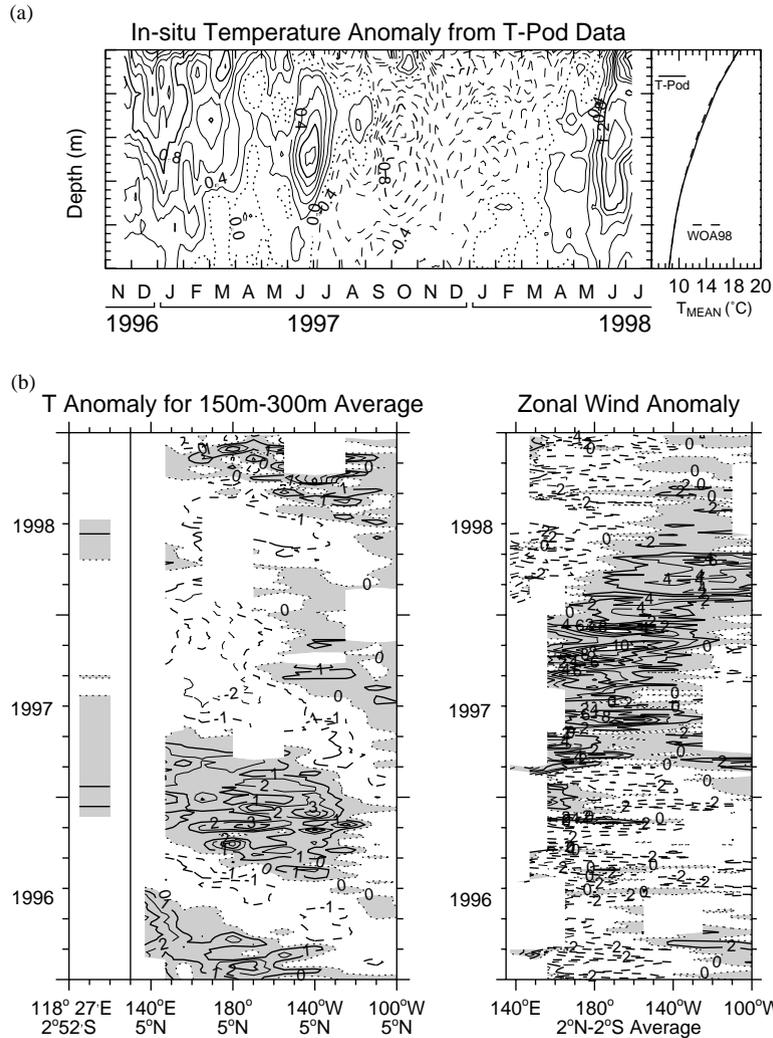
Fig. 12. (a) In situ temperature anomaly from T-pods attached to MAK1 mooring as a function of time and depth. Anomalies are relative to the NODC's WOA98 annual mean, which is plotted on the r.h.s. along with T-pod time series mean, (b) Time series of temperature anomaly averaged between 150 and 300 m from T-pod data and from TAO array along 5°N across the Pacific Ocean (left-hand panel), and of equatorial zonal wind anomaly (right-hand panel); contour interval is 0.5°C and 1 m s^{-1}, respectively, and positive and eastward anomalies, respectively, are shaded gray.

record in January 1986, as expected during an El Niño event.

4. Concurrent temperature data

T-pods located on the MAK1 mooring (Ffield et al., 2000) only spanned a depth range of 150–400 m, so captured little of the seasonal

signal. A significant interannual (or longer time-scale) signal was captured (Fig. 12), and the mean profile from the T-pod data agrees well with that obtained from NODC's World Ocean Atlas 1998 (Antonov et al., 1998). The signal in Fig. 12a is characterized by positive temperature anomalies above 300 m from the start of the time series in November 1996 until June 1997, then negative anomalies through until April 1998, after which

the anomalies are positive again. Following Clarke (1991), these anomalies can be interpreted as resulting from the transmission into the archipelago of warm, downwelling Rossby waves during the 1995/1996 La Niña, then cool, upwelling Rossby waves during the El Niño of 1997/1998 used to interpret the low-frequency transport signal in Fig. 8. The abrupt cessation of the El Niño in June 1998, and the ensuing La Niña, is well captured by the return of warm anomalies. The connection is highlighted by the time series from the Pacific TAO array shown in Fig. 12b. Subsurface temperature anomalies are shown propagating westwards along 5°N in the left-hand panel of Fig. 12b. Their arrival at the western boundary is followed almost immediately by their appearance in Makassar Strait; the temperature anomalies measured by the T-pods have been plotted alongside. The amplitude in Makassar Strait is only a fraction of that in the west Pacific, as expected from Clarke's theory. Clarke (1991) estimated that the fractional amplitude was about 15% for a first-horizontal mode Rossby wave. The corresponding equatorial zonal wind anomalies in the Pacific are shown in the right-hand panel of Fig. 12b. In simple terms, a patch of anomalous westerlies generates eastward-propagating, warm, downwelling equatorial Kelvin waves, and westward-propagating, cold, upwelling equatorial Rossby waves, and vice versa for anomalous easterlies.

5. Summary and discussion

Monthly averaged current meter data from two moorings in Makassar Strait from the end of November 1996 through mid-July 1998 show several remarkable features, notably a mean northward flow at depths below 800 m of about 5 cm s^{-1} with an r.m.s. variability of 10 cm s^{-1}. Between 800 and 250 m, the mean current is southward, but there is intense variability between 300 and 400 m. Northward anomalies reach 25 cm s^{-1}, and southward anomalies 30 cm s^{-1}. The northward anomalies are also associated with an intense vertical shear over these depths. The mean current recorded at the western mooring is

typically larger than that at the eastern one consistent with a western boundary layer width of about 70 km. A similar relationship holds for the anomalies, except during monsoon transition months when the current is apparently more western-intensified, suggesting coastal-trapped signals propagating in opposite directions through the Strait. Based on the MAK1 data, the 12-month mean southward transport over the depths covered by the current meters, i.e. 260–1500 m for 1997, is about 2.9 Sv with a maximum southward transport in March 1997 of about 7.8 Sv, and a maximum northward transport in October 1997 of 2.8 Sv; the transport averaged over these depths is northwards for 4 of the 12 months.

For climate issues, and the throughflow's impact on the Indian Ocean, though, the question is how much transport occurred over the upper thermocline, specifically how much did it add to the mean given by the data, and how much did it add or alter the variability? Gordon and Susanto (1999) and Gordon et al. (1999) attempted to answer this question by considering three empirical extrapolations to the data. Here, two sets of classic normal vertical modes for the Strait are fitted to the data. The first set is calculated using the climatological mean buoyancy frequency profile, and the second from the average of a series of high-resolution CTD casts taken in July/August 1993. The two sets of normal modes chosen have different characteristics. Those from the climatological mean profile are more surface trapped yielding a large amplitude for the first baroclinic mode at the surface, and the higher extrema of the second and third baroclinic modes lie above the depths captured by the current meter data. The other set of normal modes have deeper extremea and zero crossings, and the extremea for the second and third baroclinic mode lie within the data range. The success with which these modes can be fitted to the data, and the result provide a realistic picture of the flow at depths outside the data range, depends on whether the extremea captured by the data in Figs. 5 and 6 are the major ones, or just subsidiary ones.

The first three baroclinic normal modes were fitted sequentially, and the order in which they were fitted permuted, so that the spread amongst

the results from the permutations serves as an error estimate. Tests with almost full-depth LADCP profiles from Makassar Strait, and the current meter data, suggested that the less surface-trapped set of modes gave a better fit. However, the larger error bars on the more surface-trapped modes enabled the values from the actual LACDP profile (before it was linearly interpolated between 500, 750 and 1500 m to mimic the treatment of the current meter data) to be included. Also, including the three months of ACDP data on the MAK2 mooring between 20 and 200 m improved the fit for the more surface-trapped modes, whereas for the deeper set of modes, the revised fit lay outside the current-meter-only error bars, and was close to the values given by the other set of modes.

The normal mode fitting was carried out on each month of data, and encouragingly, the resultant transport time series looked plausible when compared with an Indonesian throughflow transport time series from a global ocean GCM hindcast in which subsurface temperature data had been assimilated. The reconstruction suggests that a significant fraction of the transport occurs in the mid-thermocline, whereas the transport in the GCM was mainly confined to the upper thermocline. A likely explanation for the difference in vertical transport distribution is that the GCM bathymetry did not resolve the 600 m sill at the southern end of Makassar Strait, which likely influences the flow at depth through the JEBAR (Joint Effect of Baroclinicity and Relief) effect. Waworuntu et al. (2001) in an examination of data collected from deep inverted echo sounders with pressure gauges in Makassar Strait from November 1966 to February 1998, TOPEX altimeter data and the MAK current meter data, also concluded that at least a three-layer system was required to give a consistent explanation of the resultant time series; the surface layer was the most energetic, though the thick middle layer contributed significantly to the transport variations.

In conclusion, the normal-mode-reconstruction method gives an estimated mean *net* transport for 1997 of 6.4 Sv southwards with upper and lower bounds of 16.0 and 4.7 Sv respectively, which compares with Gordon et al.'s (1999) estimate of 9.3 Sv with upper and lower bounds of 11.3 and 6.6 Sv; neither method gives definitive bounds on the estimate. Over the upper 250 m, the estimated mean transport for 1997 is 2.0 Sv southwards with upper and lower bounds of 9.7 and 0.8 Sv, respectively. The range of the 20-month trend in net transport is estimated to lie between 7.5 and 12.4 Sv. The transport and temperature trends are consistent with the notion of a cessation in the Trades over the equatorial Pacific and the propagation of cool, upwelling Rossby waves through the Strait as the 1997/1998 ENSO develops, as traced by concurrent temperature data from T-pods on the MAK1 mooring, and wind-stress and temperature from TAO data in the equatorial Pacific Ocean.

Acknowledgements

References

Anderson, D.L.T., Gill, A.E., 1975. Spin-up of a stratified ocean, with application to upwelling. Deep-Sea Research 22, 583–596.

Antonov, J., Levitus, S., Boyer, TP., Conkright, M., O'Brien, T., Stephens, C., 1998. World Ocean Atlas 1998, Vol. 2. Temperature of the Pacific Ocean. NOAA Atlas NESDIS, 28. US Government Printing Office, Washington, DC, 166pp.

Aung, T.H., 1995. Indo–Pacific throughflow and its seasonal variations. In: Cresswell, G., Wells, G. (Eds.), Proceedings of the ASEAN-Australia Regional Ocean Dynamics Expeditions 1993–1995. Symposium in Lombok, Australian Marine Science and Technology Limited, 26–29 June 1995.

Boyer, T.P., Conkright, M.E., Levitus, S., Stephens, C., O'Brien, T., Johnson, D., Gelfeld, R., 1998a. World Ocean Database 1998, Volume 4. Temporal distribution of conductivity/salinity-temperature-depth (Pressure) Stations.

NOAA Atlas NESDIS, Vol. 21. US Government Printing Office, Washington, DC, 160pp.

Boyer, T.P., Conkright, M.E., Levitus, S., Johnson, D., Antonov, J., O'Brien, T., Stephens, C., Gelfeld, R., 1998b. World Ocean Database 1998, Volume 5. Temporal Distribution of Station Data Temperature and Salinity Profiles. NOAA Atlas NESDIS, Vol. 22. US Government Printing Office, Washington, DC,108pp.

Boyer, T.P., Levitus, S., Antonov, J., Conkright, M., O'Brien, T., Stephens, C., 1998c. World Ocean Atlas 1998, Volume 5. Salinity of the Pacific Ocean. NOAA Atlas NESDIS, Vol. 31, US Government Printing Office, Washington, DC, 166pp.

Chow, V.T., 1959. Open-channel Hydraulics. McGraw-Hill, New York, 680 pp.

Clarke, A.J., 1991. On the reflection and transmission of low-frequency energy at the irregular western Pacific Ocean boundary. Journal of Geophysical Research 96, 3289–3305.

Ffield, A., Vranes, K., Gordon, A.L., Susanto, R.D., 2000. Temperature variability within Makassar Strait. Geophysical Research Letters 27, 237–240.

Gill, A.E., 1982. Atmosphere-Ocean Dynamics. Academic Press, New York, 662pp.

Gordon, A.L., Fine, R., 1996. Pathways of water between the Pacific and Indian Oceans in the Indonesian seas. Nature 379 (6561), 146–149.

Gordon, A.L., Susanto, R.D., 1999. Makassar Strait transport. Initial estimate based on ARLINDO results. MTS Journal 32, 34–45.

Gordon, A.L., Susanto, R.D., Ffield, A., 1999. Throughflow within Makassar Strait. Geophysical Research Letters 26, 3325–3328.

McCreary, J.P., 1981. A linear stratified model of the coastal undercurrent. Philosophical Transactions of the Royal Society of London. Series A 302, 385–413.

Murray, S.P., Arief, D., 1988. Throughflow into the Indian Ocean through Lombok Strait. January 1985–January 1986. Nature 333, 444–447.

National Oceanic and Atmospheric Administration (NOAA), 1988. ETOPO5 digital relief of the surface of the Earth, Data Announcement 88-MGG-02, National Geophysical Data Center, Boulder, Colorado.

Smith, W.H.F., Sandwell, D.T., 1997. Global sea floor topography from satellite altimetry and ship depth soundings. Science 277 (5334), 1956–1962.

Vranes, K., Gordon, A.L., Ffield, A., 2002. The heat transport of the Indonesian Throughflow and implications for the Indian Ocean heat budget. Deep-Sea Research II 49, 1391–1410.

Wajsowicz, R.C., 1996. Flow of a western boundary current through multiple straits. An electrical circuit analogy for the Indonesian throughflow and archipelago. Journal of Geophysical Research 101 (C5), 12,295–12,300.

Wajsowicz, R.C., 2002. Air–sea interaction over the Indian Ocean induced by changes in the Indonesian throughflow. Climate Dynamics 18, 437–453.

Wajsowicz, R.C., Gill, A.E., 1986. Adjustment of the ocean under buoyancy forces. Part 1. The role of Kelvin waves. Journal of Physical Oceanography 16, 2097–2114.

Waworuntu, J.M., Garzoli, S.L., Olson, D.B., 2001. Dynamics of Makassar Strait. Journal of Marine Research 59, 313–325.

Wyrtki, K., 1961. Physical oceanography of the Southeast Asian waters. NAGA Report Vol. 2. University of California, 195pp.